

Groundwater Origin and Quality Appraisal through a Combined Geochemical and Isotopic Approach in the Great Algiers District (Algeria)

Dalèle Khou

Algiers Nuclear Research Centre

Adnane Souffi Moulla (✉ asmoulla@gmail.com)

Algiers Nuclear Research Centre <https://orcid.org/0000-0002-0225-6769>

Mohammed El-Hocine Cherchali

Algiers Nuclear Research Centre

Hadjer Chorfi

Algiers Nuclear Research Centre

Mounia Benchabane

Algiers Nuclear Research Centre

SidAli Ouarezki

Algiers Nuclear Research Centre

Messaouda Belaid

Algiers Nuclear Research Centre

Research Article

Keywords: Great Algiers district, Groundwater, Mitidja basin, Hydrogeochemistry, Water Isotope, Tritium

Posted Date: May 7th, 2021

DOI: <https://doi.org/10.21203/rs.3.rs-494956/v1>

License: © ⓘ This work is licensed under a Creative Commons Attribution 4.0 International License.

[Read Full License](#)

Groundwater Origin and Quality Appraisal through a Combined Geochemical and Isotopic Approach in the Great Algiers District (Algeria)

D. Khouss, A.S. Moulla*, M. E-H. Cherchali, H. Chorfi, M. Belaid, S. Ouarezki, M. Benchabane

Algiers Nuclear Research Centre, Dating and Isotope Tracing Department, 02, Bd. Frantz Fanon, P.O. Box 399, Alger-RP, 16000, Algiers, Algeria.

*Corresponding author: A.S. Moulla, asmoulla@gmail.com, [ORCID: 0000-0002-0225-6769](https://orcid.org/0000-0002-0225-6769)

Abstract

The assessment of the origin of water that is allocated both for people and for irrigation in the eastern part of the Mitidja plain was carried out making use of geochemical and isotopic tools (^{18}O , ^2H and ^3H). Both hydrochemical and isotopic information gathered for eastern Mitidja alluvial aquifer were used for the sake of assessing the mechanisms controlling groundwater chemistry. This allowed one to identify: (i) the natural or the anthropogenic processes that control groundwater quality, (ii) the origin of groundwater and when its recharge occurs. The work involved sampling campaigns, in situ measurements, and analyses of ions, heavy metals and water isotope content. Results showed a fair overall chemical quality of waters, since the assessment of water quality using water quality index (WQI) revealed that 90 % of the groundwater samples are good. Mitidja's groundwaters fall into the $\text{Cl-SO}_4\text{-Ca}$ water type, that is mainly induced by water-rock interactions (dissolution of evaporites). The concentrations in Fe, Mn, Ni and Cd for some of the samples were found higher than the prescribed limits recommended by the World Health Organization. Isotopes indicate that groundwater is young since it originates from direct infiltration of precipitation that is mostly induced by Mediterranean atmospheric disturbances.

Keywords Great Algiers district, Groundwater, Mitidja basin, Hydrogeochemistry, Water Isotope, Tritium.

1. Introduction

North-Africa and the Maghreb region are experiencing since several decades a water deficit and are expected to lack acceptable quality water by 2025. In Algeria, the issue of water's availability is of a major concern for the water sector. Great efforts are nowadays directed towards ensuring water allocation to people but also to sustain agriculture as the resource becomes scarcer with time (Nezzal and Iftini Belaid 2013; Mimouni and Chibane 1989). Moreover, surface and groundwater, are both facing a deterioration of their quality mainly induced by natural and anthropogenic pollution. Taking into account climate change, availability of good quality water on a long-term scale is foreseen to be drastically impacted. Presently, the main concern for local authorities is to satisfy the water demand of all the sectors (population, agriculture and industry). Algiers the capital city of Algeria is considered as the largest agglomeration of the country. It experiences a fast demographic growth and a significant modernization of its industry and agriculture. It occurs on the Mediterranean coast in the Mitidja basin that comprises an important aquifer that has been used for long time. It is considered as the main source of water for

the whole very north central part of the country. The aquifer has experienced many problems due to its overexploitation (drawdown, seawater intrusion, pollution, etc.). Urban and industrial effluents together with the use of fertilizers and pesticides have also contributed to the degradation of water quality and have seriously affected the efficiency of water allocation programs (Imerzoukene and Walraevens 1999; Hadjoudj et al. 2014).

The present study aimed at enhancing the current knowledge and the status of the groundwater resources that are exploited in the region of interest. It targeted the identification of the origin and the characterization of the quality of the tapped groundwater by means of chemical and isotopic tools. Both geochemical and isotopic data related to Mitidja's alluvial aquifer were interpreted in order to characterize the mechanisms that control chemistry. Such an approach has led to the identification of natural and/or anthropogenic processes that govern groundwater quality, as well as the source, the origin and the timing of the recharge.

2. Regional setting

The investigated area is the most expanded sub-littoral Algerian plain. It is oriented East–West in the very central north of Algeria and extends over a length of 80 km and a width of 10–20 km. It covers a surface-area of 1450 km². It is limited by the Mediterranean Sea to the north, the Blidean Atlas to the south, wadi Menaceur watershed to the west, and Reghaia wadi to the east (**Fig. 1**). It is divided into four sub-watersheds. From south to north these sub-watersheds are: Nador, Mazafran, El-Harrach and the eastern sub-watershed (wadi El-Hamiz and wadi Reghaia) (Benziada 2003). It is characterized by a Mediterranean climate with an average rainfall of ~660 mm/year.

Mitidja plain is an alluvial basin formed by a coastal land subsidence that was followed by an active sedimentation phase. Two main superimposed aquifers are to be considered underground:

- The confined Eocene's aquifer is formed by Pliocene' sandstones and sandy limestones. Its substratum is composed of Pleistocene' blue marls and its roof by semi-permeable yellow marls named El-Harrach's marls. Its average thickness varies from 100 to 150 m. This aquifer is deep and lays generally between 250 and 300 m below ground surface in the major part of the plain. It is thus naturally less vulnerable to pollution compared to the quaternary phreatic aquifer (Altine-Samey and Gang 2008).
- The Quaternary alluvial aquifer is mainly composed of sands, gravels alternating with silts and clays. Apart from Mazafran's area in the west, this aquifer is entirely unconfined and lies on El-Harrach's yellow marls. Its thickness varies from 100 to 200 m. Its eastern and western limits are ensured by the uplifting of the Pleistocene' blue marls. This aquifer whose piezometric level varies between 4 and 30 m is the main

groundwater reservoir for the region. Its recharge originates mainly from rainfall, but also from the infiltrations through the beds and banks of the wadis that flow in that area.

3. Materials and methods

Groundwater sampling from the Mitidja's alluvial aquifer was performed in March 2017 for physico-chemical, heavy metals, stable isotopes ($\delta^{18}\text{O}$, $\delta^2\text{H}$) and tritium (^3H) (Fig. 1). The geographical locations of the sampling points were recorded via a global positioning system (GPS) receiver at the time of sample collection, as illustrated in Table 1.

Table 1 Location and in situ parameters measured of groundwater sampling sites in the Mitidja plain

Sample	Locality	Easting	Northing	pH	Temp. °C	EC μS/cm	DO		SiO ₂ mg/L
MTJ ₁	Rouiba	3°19'16.50"	36°43'34.26"	7.16	21.2	1820	7.0	13.70	
MTJ ₂	Rouiba	3°18'49.86"	36°43'13.74"	7.32	20.9	2080	7.4	13.50	
MTJ ₃	Rouiba	3°18'06.30"	36°43'30.84"	7.27	21.4	1416	5.9	13.90	
MTJ ₄	Rouiba	3°18'07.14"	36°43'53.28"	7.29	22.6	1553	7.9	14.70	
MTJ ₅	Rouiba	3°16'44.08"	36°44'07.80"	7.19	22.8	1141	6.9	14.00	
MTJ ₆	Oued Smar	3°10'12.36"	36°41'56.04"	7.34	22.0	1279	6.0	13.00	
MTJ ₇	Oued Smar	3°09'59.22"	36°42'06.42"	7.15	22.6	1356	5.5	12.69	
MTJ ₈	Oued Smar	3°10'20.64"	36°41'44.52"	7.18	18.0	2120	8.0	13.09	
MTJ ₉	Oued Smar	3°11'04.98"	36°41'45.84"	7.60	23.3	1263	7.8	13.58	
MTJ ₁₀	Oued Smar	3°11'11.46"	36°41'45.90"	7.46	21.0	1185	3.1	12.52	
MTJ ₁₁	Oued Smar	3°11'23.04"	36°41'48.18"	7.47	18.9	1400	5.6	12.05	
MTJ ₁₂	Oued Smar	3°10'08.58"	36°41'46.74"	7.42	21.2	1090	6.9	13.76	
MTJ ₁₃	Dar El Beida	3°12'43.80"	36°43'17.34"	6.90	20.5	1460	5.4	12.57	
MTJ ₁₄	Dar El Beida	3°13'15.54"	36°43'08.34"	7.10	20.7	1180	7.6	12.93	
MTJ ₁₅	Dar El Beida	3°12'22.26"	36°43'03.90"	6.90	21.1	1480	5.7	13.00	
MTJ ₁₆	Dar El Beida	3°12'34.38"	36°43'10.26"	7.00	21.0	1538	2.2	13.02	
MTJ ₁₇	Dar El Beida	3°12'48.84"	36°43'13.86"	7.04	21.5	1293	4.8	13.06	
MTJ ₁₈	Reghaia	3°17'45.00"	36°42'58.56"	7.06	20.2	1425	8.4	12.89	
MTJ ₁₉	Reghaia	3°19'26.40"	36°44'12.26"	7.00	21.5	1507	6.5	13.01	
MTJ ₂₀	Reghaia	3°19'42.96"	36°44'08.40"	6.90	21.0	1431	6.3	13.71	

Major elements (Ca^{2+} , K^+ , Na^+ , Mg^{2+} , NO_3^- , SO_4^{2-} , Cl^-) were analyzed by high performance ionic liquid chromatography (HPLC, Dionex DX-120). Total alkalinity as HCO_3^- was determined by titration using 0.1N HCl. Analyses with a charge balance lower than $\pm 5\%$ were accepted. Concentrations of Fe, Mn, Ni and Cd were measured by means a single beam atomic absorption spectrophotometer (Model Perkin Elmer-AAnalyst 400). Stable isotope contents ($\delta^{18}\text{O}$, $\delta^2\text{H}$) were analyzed using a laser absorption spectrometer (Picarro L2110-i) (Penna et al. 2010). This was undertaken at the premises of the Dating and Isotope Tracing Dept. of the Algiers Nuclear Research Centre. The results are given as relative deviations (δ in per mil) from the Vienna Standard Mean Ocean Water (*V-SMOW*). Tritium content was measured at the same laboratory by low level liquid scintillation spectrometry after samples have undergone electrolytic enrichment (Taylor 2010).

Fig. 1 Map showing the geographic location and sampling sites in Mitidja's plain

4. Results and discussion

4.1 Field parameters

The results of the onsite measured physico-chemical parameters are presented in Table 1. The average of groundwaters' pH values was 7.2, which is considered as normal. These waters are within the limits of the guideline values for human consumption (WHO 2011).

Water's temperature governs solubility in particular regarding dissolved gases; it is directly related to water's origin (Boeglin 2009). It allows differentiating between deep groundwaters and those circulating near the surface. Groundwaters' temperature was relatively stable (18 to 23°C) with a mean value of 21°C. Dissolved oxygen concentrations ranged from 2.2 to 8.4 mg/L with an average of 6.2 mg/L. Values of electrical conductivity (EC) ranged from 1090 to 2120 $\mu\text{S}/\text{cm}$, with a mean value of 1451. As far as EC is concerned, 25 % of the samples exhibited results higher than the recommended values for drinking purposes.

4.2 The hydrogeochemical approach

4.2.1 Hydrochemical facies

The Piper's trilinear diagram shows that 80 % of groundwater samples fall into the $\text{Cl}/\text{HCO}_3\text{-Ca}$ type, whereas 15% are classified as $\text{HCO}_3/\text{Cl-Ca}$ facies, and remaining $\text{Cl}/\text{HCO}_3\text{-Na}$ type. Therefore, facies classification indicates that maximum groundwater samples belong to $\text{Cl}/\text{HCO}_3\text{-Ca}$ (Fig. 2). The most dominant trend for major cations is as follows: $\text{Ca}^{2+} > \text{Na}^+ > \text{Mg}^{2+} > \text{K}^+$, while for anions it is as follows: $\text{Cl}^- > \text{HCO}_3^- > \text{SO}_4^{2-} > \text{NO}_3^-$ (Table 2).

Table 2 Hydrochemical parameters of the studied groundwater samples

Sample	Ca^{2+}	Mg^{2+}	Na^+	K^+	Cl^-	SO_4^{2-}	HCO_3^-	NO_3^-	F^-	Br^-	Li^+
	(mg/L)										
MTJ ₁	167.90	27.31	172.62	4.66	396.34	127.26	316.42	35.77	0.51	3.18	0.24
MTJ ₂	206.61	46.12	196.60	5.47	449.80	170.25	302.67	95.70	0.51	3.23	0.40
MTJ ₃	162.5	39.50	102.90	4.92	320.90	123.80	253.13	38.90	0.51	2.86	0.39
MTJ ₄	175.52	39.87	108.50	4.74	352.80	157.80	251.76	29.78	0.52	2.93	0.40
MTJ ₅	155.06	35.66	88.75	4.08	236.60	127.80	233.76	30.36	0.52	2.63	0.39
MTJ ₆	145.61	38.03	129.70	3.72	223.70	135.80	316.42	4.55	0.60	2.63	0.40
MTJ ₇	145.90	36.03	117.90	4.87	200.50	136.06	302.67	32.90	0.50	2.51	0.41
MTJ ₈	205.56	67.95	230.23	4.74	471.50	211.60	302.67	2.02	0.54	3.17	0.41
MTJ ₉	129.89	36.93	106.40	4.03	236.20	97.14	269.65	12.65	0.56	2.68	0.40
MTJ ₁₀	119.21	37.72	106.08	3.33	240.08	92.08	302.67	9.44	0.63	2.69	0.40
MTJ ₁₁	131.27	46.17	136.50	3.42	294.60	98.67	302.67	7.57	0.68	2.76	0.40
MTJ ₁₂	105.39	29.70	112.80	4.04	185.80	95.60	280.65	4.04	0.56	2.56	0.41
MTJ ₁₃	180.50	44.90	100.90	3.12	156.80	185.20	423.73	30.9	0.51	2.47	0.31
MTJ ₁₄	128.53	34.25	101.30	2.68	139.11	161.40	319.17	15.80	0.54	2.42	/
MTJ ₁₅	160.40	43.42	124.90	3.29	215.16	243.09	294.41	38.08	0.56	2.43	0.30
MTJ ₁₆	151.60	41.04	125.10	2.18	209.30	182.60	310.92	38.80	0.54	2.52	/
MTJ ₁₇	146.20	38.90	92.59	2.86	165.80	140.90	310.92	21.66	0.51	2.37	0.30
MTJ ₁₈	165.80	38.74	101.24	2.62	221.50	116.50	275.15	109.60	0.57	2.46	0.30
MTJ ₁₉	163.70	41.16	125.60	3.95	241.18	146.30	280.65	40.20	0.50	2.45	0.31
MTJ ₂₀	140.81	36.90	134.00	5.02	260.68	145.90	291.66	44.30	0.52	2.44	0.32
Average	154.4	40	126	3.88	261	145	297	32	0.54	2.7	0.36

Fig. 2 Piper diagram classification of the analyzed groundwater samples

4.2.2 Origin and mechanism of groundwater mineralization

The correlations that were drawn between the concentrations of the major elements and the conductivity allowed one to determine the origin of Mitidja underground waters' mineral load. Table 3 illustrates the correlation coefficients matrix for the hydrochemical data for the studied alluvial reservoir. Ca^{2+} , Na^+ , Cl^- , SO_4^{2-} and Mg^{2+} display fairly strong positive correlations with EC indicating thus that these ions contribute significantly to groundwater mineralization.

Table 3 Correlation matrix for the investigated groundwater samples

	T°C	pH	EC	DO	Ca^{2+}	Mg^{2+}	Na^+	K^+	HCO_3^-	F^-	Cl^-	Br^-	SO_4^{2-}	NO_3^-	SiO_2	Li^+
T°C	1															
pH	0.224	1														
EC	-0.062	-0.162	1													
DO	0.098	0.149	0.244	1												
Ca^{2+}	0.058	-0.336	0.857	0.313	1											
Mg^{2+}	-0.430	-0.093	0.618	0.080	0.616	1										
Na^+	-0.175	0.048	0.881	0.243	0.596	0.598	1									
K^+	0.376	0.247	0.446	0.421	0.364	0.095	0.488	1								
HCO_3^-	-0.274	-0.351	0.150	-0.310	0.141	0.165	0.119	-0.322	1							
F^-	-0.395	0.526	-0.285	-0.209	-0.470	0.091	-0.040	-0.364	-0.002	1						
Cl^-	0.022	0.257	0.837	0.362	0.660	0.479	0.818	0.687	-0.238	-0.086	1					
Br^-	-0.179	-0.119	0.025	0.343	0.140	-0.016	-0.115	-0.282	-0.146	0.127	-0.040	1				
SO_4^{2-}	-0.141	-0.656	0.526	-0.020	0.617	0.551	0.381	-0.048	0.320	-0.365	0.155	-0.168	1			
NO_3^-	0.325	-0.346	0.353	0.231	0.478	-0.045	0.066	0.076	-0.104	-0.323	0.180	0.665	0.127	1		
SiO_2	0.473	0.105	0.087	0.434	0.175	-0.266	-0.023	0.537	-0.577	-0.512	0.339	-0.111	-0.031	0.106	1	
Li^+	0.183	0.496	0.048	0.271	0.102	0.196	0.137	0.605	-0.280	0.163	0.356	-0.026	-0.314	-0.096	0.163	1

Significant level at $p < 0.05$

In order to determine the origin and the processes that contribute to groundwater mineralization, some relationships between major elements are discussed. The plot of Na vs. Cl (**Fig. 3a**) reflects a strong relationship between those two elements that mainly originate from the dissolution of Halite. This process is verified by the linear evolution of Halite saturation indices (SI) as depicted in **Fig. 3b**.

Fig. 3 Plots of **a** Na^+/Cl^- , **b** $(\text{Na}^+ + \text{Cl}^-)/\text{Halite SI}$

Ca^{2+} is linearly correlated with SO_4^{2-} with an excess Ca^{2+} (**Fig. 4a**) indicating the same origin for both ions (anhydrite/gypsum minerals). The effect of this dissolution is linked with the proportional evolution between the negative saturation indices of Anhydrite and Gypsum and $(\text{Ca}^{2+} + \text{SO}_4^{2-})$ (**Fig. 4 b-c**).

Fig. 4 Plots of **a** $\text{Ca}^{2+}/\text{SO}_4^{2-}$, **b** $(\text{Ca}^{2+} + \text{SO}_4^{2-})/\text{Anhydrite SI}$, **c** $(\text{Ca}^{2+} + \text{SO}_4^{2-})/\text{Gypsum SI}$

The deficit in Na^+ with respect to Cl^- and the excess of Ca^{2+} with respect to SO_4^{2-} , both indicate that cation exchange is the major chemical process taking place within the aquifer. It results in Na^+ adsorption on clay minerals and a simultaneous release of Ca^{2+} (Kuitcha et al. 2013). This process is also highlighted by the positive correlation between $\text{Ca}^{2+}/\text{Mg}^{2+}$ ratio and the excess of Ca^{2+} with respect to Na^+ (**Fig. 5 a-b**). The aforementioned ion exchange

process is also verified through the inverse proportional evolution between $(Ca^{2+} + Mg^{2+}) - (HCO_3^- + SO_4^{2-})$ and $(Na^+ + K^+ - Cl^-)$ as depicted in Fig. 6.

Fig. 5 Plots of **a** Ca^{2+}/Na^+ , **b** Ca^{2+}/Mg^{2+}

Fig. 6 Plot of $(Na^+ + K^+) - Cl^-$ vs $(Ca^{2+} + Mg^{2+}) - (HCO_3^- + SO_4^{2-})$

4.3 Water quality assessment

4.3.1 Suitability for drinking

To check the drinking suitability of groundwater, the hydrochemical features of the samples were compared to the WHO prescribed limits of WHO (WHO 2011). The mean concentrations of major cations and anions were found within the range of drinking water guidelines set by the WHO. Alluvial aquifer groundwaters exhibit a good mineral drinkability potential (Table 4).

Table 4 Mean concentrations of measured major elements

Major ions	Concentrations (mg/L)	
	WHO guideline values	Mean value
Calcium (Ca^{2+})	200	154.4
Magnesium (Mg^{2+})	150	40.0
Sodium (Na^+)	150	126.0
Potassium (K^+)	12	3.9
Sulphates (SO_4^{2-})	250	145.0
Chlorides (Cl^-)	250	261.0
Nitrates (NO_3^-)	50	32.2

4.3.2 Water quality index in the alluvial aquifer of Mitidja basin

In general, the Water Quality Index (WQI) is a statistical functional tool for simplifying, detailed and describing complex information collected from any water body which reflects the integrated influence on the overall quality variables. This index is understandable and used by decision makers, planners and the general public (Imneisi and Aydin 2016). So, WQI is one of the most successful criterion to describe water quality. Its objective is to classify waters with respect to biological, chemical and physical characteristics that define the best their possible uses for the sake of managing their allocation (Troudi et al 2020).

To get a comprehensive picture of the overall quality of groundwater in the Mitidja basin, the WQI was computed and used through three steps:

- First, each of the 12 parameters (pH, EC, DO, HCO_3^- , Cl^- , SO_4^{2-} , NO_3^- , F⁻, Ca^{2+} , Mg^{2+} , K^+ , Na^+) was assigned a weight (wi) according to its relative importance for the overall quality of drinking water (Table 2). In general, the most important weight is attributed to parameters that have critical effects on health and whose presence exceeds the limit of water drinkability (Batabyal and Chakraborty 2015). The

maximum weight 5 was assigned to nitrate (NO_3^-) and chloride (Cl^-) because of their major importance in water quality assessment. It is noted that chloride ions exhibit high concentrations (most probably due to seawater intrusion). The lowest weight factor 1 was assigned to K^+ because of its lower importance in the determination of groundwater mineralization. Other parameters such as pH, EC, DO, HCO_3^- , SO_4^{2-} , F^- , Ca^{2+} , Mg^{2+} , F^- were assigned weights ranging between 1 and 5 based on their relative significance in the water quality assessment.

- Second, the relative weight (W_i) for the considered chemical parameter was computed using the following equation:

$$W_i = w_i / \sum_{i=1}^n w_i \quad (\text{Eq.1})$$

Where:

W_i is the relative weight;
 w_i is the weight for each parameter;
 n is the number of parameters.

Calculated relative weight values (W_i) for each parameter are illustrated in Table 5.

Table 5 Weight (w_i) and relative weight (W_i) for the chemical parameters

Chemical Parameter	WHO (2011)	Weight (w_i)	Relative weight (W_i)
pH	8.5	4	0.1026
EC	1500	4	0.1026
DO	5	2	0.0513
Ca^{2+}	200	4	0.1026
Mg^{2+}	150	3	0.0769
Na^+	150	3	0.0769
K^+	12	1	0.0256
Cl^-	250	5	0.1282
SO_4^{2-}	250	4	0.1026
HCO_3^-	280	2	0.0513
NO_3^-	50	5	0.1282
F^-	1.5	2	0.0513
		$\sum w_i=39$	$\sum W_i=1$

- In the final phase, a quality rating scale (q_i) for each parameter is assigned by dividing its concentration in each water sample by its respective standard as set by the WHO (2011), and the result is multiplied by 100 according to the following equation:

$$q_i = (C_i / S_i) \times 100 \quad (\text{Eq.2})$$

Where,

q_i is the quality rating;
 C_i is the concentration of each chemical parameter in each alluvial aquifer sample in mg/L;
 S_i is the drinking water standard set by the WHO (2011) for each chemical parameter in mg/L;

In order to compute the WQI, the subindex (SI) is first determined for each chemical parameter, as given by equation (Eq.3):

$$SI_i = W_i \times q_i \quad (\text{Eq.3})$$

$$WQI = \sum SI_{i-n} \quad (\text{Eq.4})$$

Where:

SI_i is the sub index of i^{th} parameter;

W_i is the relative weight of i^{th} parameter;
 q_i is the rating based on concentration of i^{th} parameter;
 n is the number of chemical parameters.

The obtained results are compared and summarized in the following five (5) classes (**Table 6**):

Table 6 WQI classes and water quality type

WQI value	Rating of water quality	Number of water samples
WQI<50	Excellent	0
50<WQI<100	Good	18
100<WQI<200	Poor	2
200<WQI<300	Very poor	0
WQI>300	Unsuitable for drinking purposes	0

The values of the computed WQI and water type of the individual samples are presented in Table 7. The WQI ranges from 60.75 to 119.36 with a mean value of 79 (**Fig. 7**).

The application of the WQI shows that 90 % of the groundwater samples are good while the remaining 10% are poor. The dissolved ions affected WQI values in samples 2 and 8, particularly Ca^{2+} , Na^+ , Cl^- , SO_4^{2-} , and NO_3^- in sample 8. The poor quality is verified by high values of conductivity in samples 2 and 8 which exhibited 2080 and 2120 $\mu\text{S}/\text{cm}$ respectively. The degradation of water quality is linked to the impact of agricultural activities and in particular to the excessive use of nitrogenous fertilizers (sample 2: $\text{NO}_3^- = 95.7 \text{ mg}/\text{L}$) but also to marine intrusion. Regarding the latter, high chloride and sodium concentrations are observed in samples 2 and 8: 449.8 and 471.5 mg/L for chloride and 196.6 then 230.2 mg/L for sodium respectively.

Table 7 Computation of the Water Quality Index (WQI) for individual groundwater samples

Sample	WQI	Water type
MTJ₁	93.16	Good
MTJ₂	119.36	Poor
MTJ₃	81.12	Good
MTJ₄	85.78	Good
MTJ₅	71.48	Good
MTJ₆	68.33	Good
MTJ₇	73.68	Good
MTJ₈	101.06	Poor
MTJ₉	68.93	Good
MTJ₁₀	62.43	Good
MTJ₁₁	71.87	Good
MTJ₁₂	60.75	Good
MTJ₁₃	75.60	Good
MTJ₁₄	65.62	Good
MTJ₁₅	81.49	Good
MTJ₁₆	75.33	Good
MTJ₁₇	65.92	Good
MTJ₁₈	95.71	Good
MTJ₁₉	80.61	Good
MTJ₂₀	81.74	Good

Fig. 7 Water Quality Index map of the alluvial aquifer of the Mitidja plain

4.3.3 Assessment of heavy metals' contamination

Current knowledge on heavy metals' contamination is overriding due to their potential harms to the aquatic environment and human beings (Lee et al. 2007). The extent of heavy metal groundwater contamination in the study area was assessed by comparison with the WHO guidelines for drinking purposes (WHO 2011). Groundwater concentrations for four heavy metals namely: Cd, Mn, Fe and Ni have been measured (Table 8).

Table 8 Trace metals concentration of groundwater samples

Sample	Cd	Ni	Fe	Mn
	(mg/L)			
MTJ ₆	0.002	0.060	0.401	0.491
MTJ ₇	0.010	0.013	0.010	0.010
MTJ ₉	0.010	0.071	0.010	0.010
MTJ ₁₀	0.029	0.112	0.010	0.010
MTJ ₁₁	0.010	0.095	0.010	0.010
MTJ ₁₂	0.003	0.021	0.070	0.010

Iron values varied from 0.010 to 0.407 mg/L with a mean value of 0.085 mg/L. As it can be seen, sample MTJ₆ content exceeded the WHO guideline for drinking water (0.2 mg/L).

Manganese concentrations ranged between 0.010 mg/L to 0.491 mg/L with an average content of 0.090 mg/L. Sample MTJ₆ content also exceeded the WHO permissible level (0.05 mg/L) (WHO 2011).

Cadmium results varied between 0.002 and 0.029 mg/L with an average concentration of 0.011 mg/L. It can also be seen that Cd contents for four groundwaters samples (MTJ₇, MTJ₉, MTJ₁₀, MTJ₁₁) exceeded the WHO permissible limit (10 µg/L).

Nickel concentrations ranged between 0.013 and 0.112 mg/L with a mean value of 0.062 mg/L with three groundwater samples (MTJ₉, MTJ₁₀, MTJ₁₁) exceeding the WHO guideline (0.07 mg/L).

Heavy metals contamination of groundwater is a result of human activities. Anthropogenic sources include agricultural practices (use of fertilizers), and both sewage and industrial effluents (Mimouni et al. 2015). Wastewater containing heavy metals and harmful compounds from many industrial discharges such as: smelting, refining, manufacturing processes, steel and textile industry, electro-plating, nickel-cadmium batteries manufacturing, welding, PVC products and paint pigments production, are all potential polluters. Such effluents with excess heavy metals may seep into the unsaturated zone of the soil and thus contaminate groundwaters.

4.4 The isotopic approach

4.4.1 Isotope composition of groundwaters

The stable isotopes of oxygen and hydrogen have conservative properties and provide information on the origin and the movement of groundwater. This approach can offer an evaluation of physical processes affecting water masses, such as evaporation and mixing (Trabelsi et al. 2012).

$\delta^{18}\text{O}$ and $\delta^2\text{H}$ values for groundwaters ranged from -6.57 to -5.85‰ and -37.9 to -33.7‰ vs V-SMOW standard respectively (Table 6). The mean isotopic composition of samples (-6.2 ‰ for $\delta^{18}\text{O}$ & -35.7 ‰ for $\delta^2\text{H}$ with a mean deuterium excess of 14.1) is close to the mean value for precipitation recorded in Algiers during the 2016-2018 period of time. As a matter of fact, it is -6.3 ‰ for $\delta^{18}\text{O}$ and -36.1 ‰ for $\delta^2\text{H}$ (unpublished data).

All points are distributed along the Meteoric Water Line for the western Mediterranean region whose deuterium excess is 14 (WMWL: $\delta^2\text{H} = 8 \delta^{18}\text{O} + 14$) (Fig. 8), as determined by Celle-Jeanton and collaborators (Celle-Jeanton et al. 2001). They are far below the eastern Mediterranean one whose deuterium excess is equal to 22 (Gat and Carmi 1970). The points lie above the Global Meteoric Water Line (GMWL: $\delta^2\text{H} = 8 \delta^{18}\text{O} + 10$) for precipitation of oceanic origin (Craig 1961). This indicates thus that the recharge of the alluvial aquifer in the plain takes part through the infiltration of recent precipitation originating mainly from western Mediterranean vapor masses (Khous et al. 2019). The mean deuterium excess for the whole set of points (14.1) is very close to that of the WMWL which is indeed another indication of the origin of groundwater.

Fig. 8 $\delta^{18}\text{O}$ – $\delta^2\text{H}$ plot for groundwater samples from the studied area

4.4.2 Tritium

For several decades, the use tritium has been regarded as the simplest and the most convenient tracing method for determining young groundwater ages (Dulinski et al. 2003). The occurrence of tritium in groundwater indicates the extent of migration of modern post-1950s recharge, but its use is limited by its short half-life (12.32 years) (Edmunds and Smedley 2000). Tritium content in groundwater depends primarily on the initial atmospheric concentration at the time of recharge and the radioactive decay that has occurred since water has infiltrated the aquifer (Farid et al. 2013).

Tritium concentrations in analyzed groundwaters are overall higher than 1 TU, with a mean value of 2.2 TU (Table 9). The presence of measurable concentrations of tritium reflects and confirms again the presence of modern infiltrated waters in the Mitidja basin (Clark et al. 1997).

Table 9 Stable isotopes and Tritium contents of Mitidja's groundwater

Sample name	$\delta^{18}\text{O}$ (‰) vs. V-SMOW	$\delta^2\text{H}$	d_{ex}	^3H (TU)
MTJ ₁	-6.11	-36.8	12.1	-
MTJ ₂	-6.08	-34.3	14.3	2.5
MTJ ₃	-6.32	-35.8	14.8	2.3
MTJ ₄	-6.13	-34.7	14.3	2.0
MTJ ₅	-6.26	-35.3	14.8	-
MTJ ₆	-6.57	-37.9	14.7	1.7
MTJ ₇	-6.34	-35.1	15.6	3.0
MTJ ₈	-6.10	-35.1	13.7	1.4
MTJ ₉	-6.33	-36.2	14.4	1.9
MTJ ₁₀	-6.32	-37.5	13.1	2.6
MTJ ₁₁	-6.33	-35.2	15.4	0.0
MTJ ₁₂	-5.95	-33.7	13.9	2.2
MTJ ₁₃	-6.31	-36.9	13.6	5.2
MTJ ₁₄	-5.93	-33.9	13.5	3.3
MTJ ₁₅	-6.18	-35.5	13.9	-
MTJ ₁₆	-6.20	-35.8	13.8	1.6
MTJ ₁₇	-6.40	-35.9	15.3	1.1
MTJ ₁₈	-5.85	-33.7	13.1	3.1
MTJ ₁₉	-6.15	-35.0	14.2	2.5
MTJ ₂₀	-6.12	-35.8	13.2	1.9
Average	-6.20	-35.5	14.1	2.2

5. Conclusion

Based on the results of the present investigation, it can be concluded that:

- Groundwaters from the quaternary alluvial aquifer in the eastern corner of the Mitidja plain are dominated by the Cl–SO₄–Ca facies that is mainly derived from the dissolution of evaporate minerals (Halite, Anhydrite/Gypsum) and exchange processes. Moreover, they exhibit good drinkability features from the mineralization viewpoint.
- Concentrations in Cd, Ni, Mn and Fe for some samples were found higher than the safe recommended values for drinking purposes as established by the WHO. These are thought to originate from anthropogenic activities (point source pollution from both industry and agriculture).
- Environmental stable isotopes (¹⁸O, ²H) results revealed the presence of waters originating from the infiltration of recent precipitation that is mainly derived from west-Mediterranean vapor masses.
- Tritium results confirmed the modern water recharge pattern of the groundwaters that occur within the alluvial aquifer of the Mitidja.

References

- Altine-Samey A, Gang C (2008) A GIS based drastic for the assessment of groundwater vulnerability to pollution in west Mitidja: Blida city, Algeria. *Research Journal of Applied Sciences* 3 (7): 500–507.
- Batabyal AK, Chakraborty S (2015) Hydrogeochemistry and Water Quality Index in the assessment of Groundwater Quality for Drinking Uses. *Water Environment Research* 87(7): 607-617. <http://DOI: 10.2175/106143015X14212658613956>.
- Benziada M. (2003) Hydrogéologie de la plaine de la Mitidja orientale (Algérie), *Bulletin des Sciences Géographiques* N°11.
- Boeglin JC (2009) Contrôle des eaux douces et de consommation humaine. Ed. *Techniques de l'Ingénieur*, p. 4210.
- Celle-Jeanton H, Travi Y, Blavoux B (2001) Isotopic typology of the precipitation in the western Mediterranean region at the three different time scales. *Geophysical Research Letters* 28: 1215–1218. <https://doi.org/10.1029/2000gl012407>
- Clark ID, Fritz P (1997) *Environmental Isotopes in Hydrology*. Lewis Publishers, Boca Raton, USA.
- Craig H (1961) Isotopic variation in meteoric water. *Science* 133:1702–1703. <https://doi.org/10.1126/science.133.3465.1702>
- Dulinski M, Rozanski K, Kania J, Karlikowska J, Korczynski-Jackowicz M, Witczak S, Mochalski P, Opoka M, Sliwka I, Zuber A (2003) Groundwater dating with Sulfur hexafluoride: Methodology and field comparison with tritium and hydrodynamic methods. *Intern. Symp.*, International Atomic Energy Agency, Vienna, Austria, IAEA-CN-104/8.
- Edmunds WM, Smedley P.L (2000) Residence time indicators in groundwater: The East Midlands Triassic sandstone aquifer. *Applied Geochemistry* 15: 737–752. [https://doi.org/10.1016/s0883-2927\(99\)00079-7](https://doi.org/10.1016/s0883-2927(99)00079-7)
- Farid I, Trabelsi R, Zouari K., Beji R (2013) Geochemical and isotopic study of surface and groundwaters in Ain Bou Mourra basin, central Tunisia. *Quaternary International* 303:210–227. <https://doi.org/10.1016/j.quaint.2013.04.021>
- Gat JR, Carmi I (1970) Evolution of the Isotopic Composition of Atmospheric Waters in the Mediterranean Sea Area. *Journal of Geophysical Research Atmospheres* 75(15): 3039–3048. <https://doi.org/10.1029/jc075i015p03039>
- Hadjoudj O, Bensemmane R, Saoud Z, Reggabi M (2014) Groundwater pollution by nitrates in the Mitidja plain: the present condition and the required corrective measures. *European Journal of Water Quality* (45):57-68.
- Imerzoukene S, Walraevens K (1999) Simulation of groundwater flow and evolution of the fresh/salt water interface in the coastal aquifer of the Mitidja plain (Algeria). *Proceedings SWIM*, Ghent :249–262.
- Imneisi IB, Aydin M (2016) Water Quality Index (WQI) for Main Source of Drinking Water (Karaçomak Dam) in Kastamonu City, Turkey. *J. Environ. Anal. Toxicol.* 6: 407. <http://doi: 10.4172/2161-0525.1000407>.
- Khous D, Ait-Amar H, Belaid M, Chorfi H (2019) Geochemical and Isotopic Assessment of Groundwater Quality in the Alluvial Aquifer of the Eastern Mitidja Plain. *Water Resources* (46): 443–453. <https://doi.org/10.1134/s0097807819030060>
- Kuitcha D, Takounjou ALF, Ndjama J (2013) Apport de l'hydrochimie et de l'isotope de l'environnement à la connaissance des ressources en eaux souterraines de Yaoundé, Cameroun. *Journal of Applied Biosciences* 67: 5194–5208. <https://doi.org/10.4314/jab.v67i0.95041>
- Lee CL, Li XD, Zhang G, Li J, Ding, AJ, Wang T (2007) Heavy metals and Pb isotopic composition of aerosols in urban and suburban areas of Hong Kong and Guangzhou, South China evidence of the long-range transport of air contaminants. *Environment. Pollution* (41): 432–447. <https://doi.org/10.1016/j.atmosenv.2006.07.035>
- Mimouni O, Chibane B (1989) Predicting nitrate pollution of Mitidja plain groundwater (Northern Algiers-Algeria). *Environmental Software*, vol. 4, No.3. 136–141. [https://doi.org/10.1016/0266-9838\(89\)90044-0](https://doi.org/10.1016/0266-9838(89)90044-0)
- Mimouni O, Cheikh Lounis G, Kabouche S, Menceur H (2015) Vulnerability to pollution of Mitidja plain alluvial aquifer (Algiers-Algeria). *International Journal of Enhanced Research in Science, Technology and Engineering*, ISSN: 2319-7463:137–143.
- Nezzal F, Ifini Belaid Z (2013) Variabilité climatique et impacts anthropiques sur la nappe alluviale de la Mitidja orientale (baie d'Alger). *Revue Scientifique et Technique, LJEE* N°21 & 22, Spécial colloque CIREDD.
- Penna D, Stenni B, Sanda M, Wrede S, Bogaard TA, Gobbi A, Borga M, Fischer BMC, Bonazza M, Chárová Z (2010) On the reproducibility and repeatability of laser absorption spectroscopy measurements for $\delta^2\text{H}$ and $\delta^{18}\text{O}$ isotopic analysis. *Hydrology and Earth System Sciences vol.14 No.8*: 1551–1566. <https://doi.org/10.5194/hess-14-1551-2010>
- Taylor CB (1977) Tritium enrichment of environmental waters by electrolysis: development of cathodes exhibiting high isotopic separation and precise measurements and applications. High Tatras, Czechoslovakia, October 1975, Bratislava.
- Trabelsi R, Abid K, Zouari K (2012) Geochemistry processes of the Djeffara palaeogroundwater (Southern Tunisia). *Quaternary International* 257: 43–55. <https://doi.org/10.1016/j.quaint.2011.10.029>

Troudi N, Hamzaoui-Azaza F, Tzoraki O, Melki F, Zammouri M (2020) Assessment of groundwater quality for drinking purpose with special emphasis on salinity and nitrate contamination in the shallow aquifer of Guenniche (Northern Tunisia), Environ. Monit. Assess. 192: 641. <https://doi.org/10.1007/s10661-020-08584-9>. World Health Organization (WHO) (2011) Guidelines for Drinking Water Quality, 4th ed., Geneva, Switzerland.

Declarations

• Funding:

Research was supported and funds were provided by the employer (governmental institution) in the framework of its normal and current activities.

• Conflicts of interest/Competing interests:

The authors who all belong to the same institution declare that there exists neither conflicts of interest nor competing interest

• Availability of data and material:

'Not applicable'

• Code availability:

'Not applicable'

• Authors' contributions:

The authors belong all to the same Lab. and then work in close co-operation, each one in its field of competence as the work is shared between them.

Figures

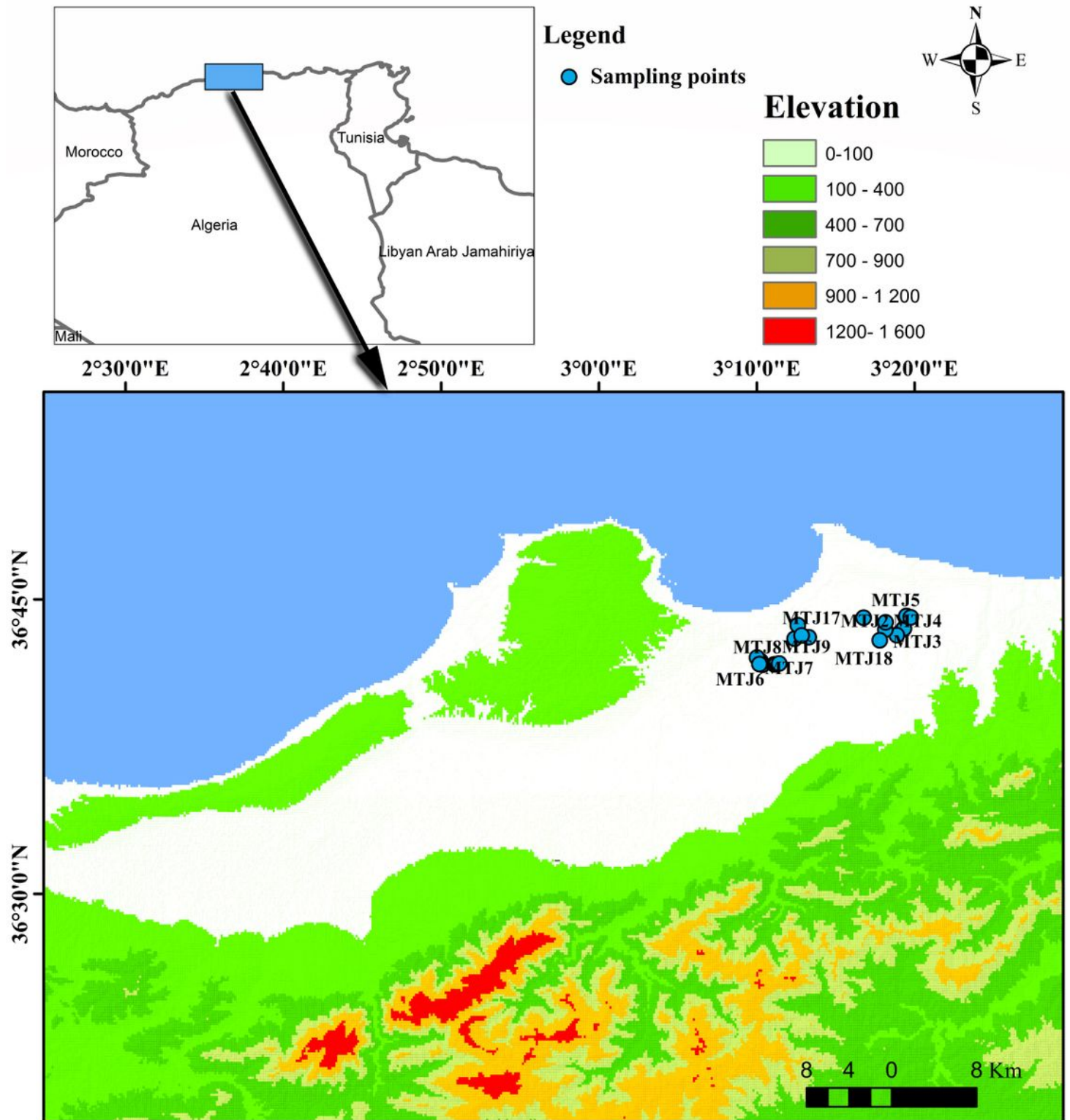


Figure 1

Map showing the geographic location and sampling sites in Mitidja's plain

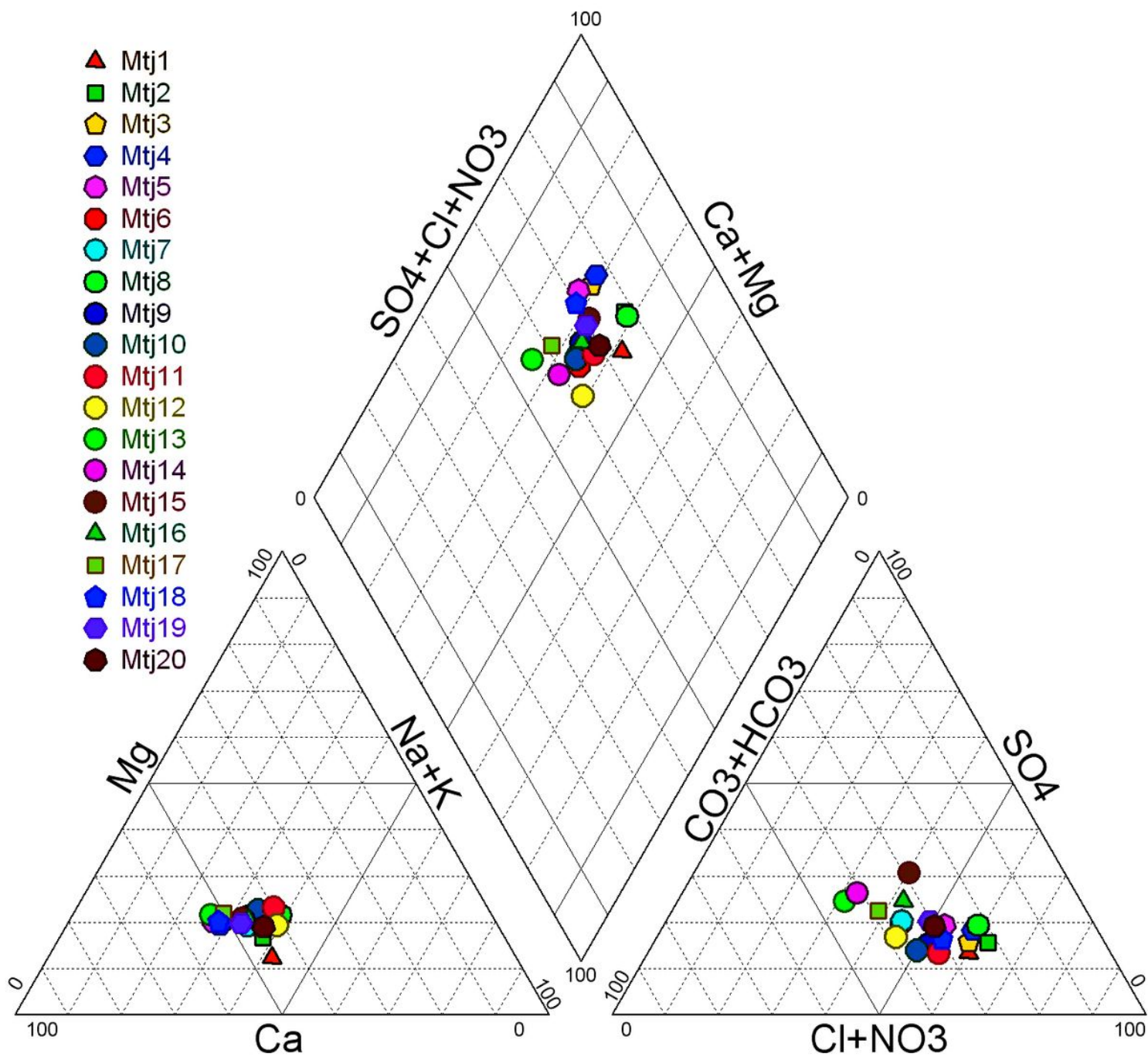


Figure 2

Piper diagram classification of the analyzed groundwater samples

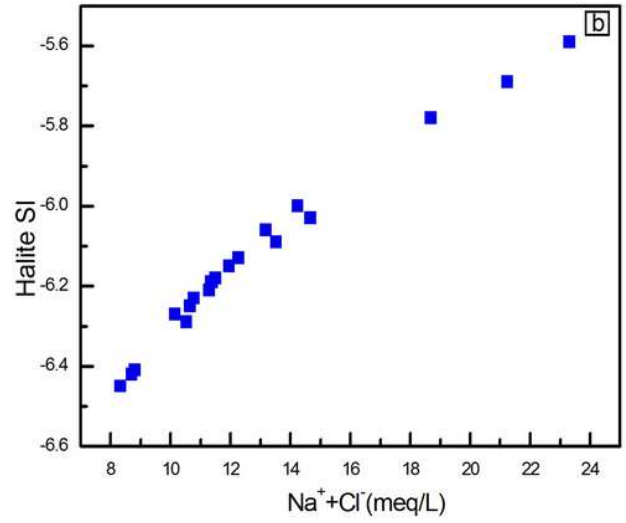
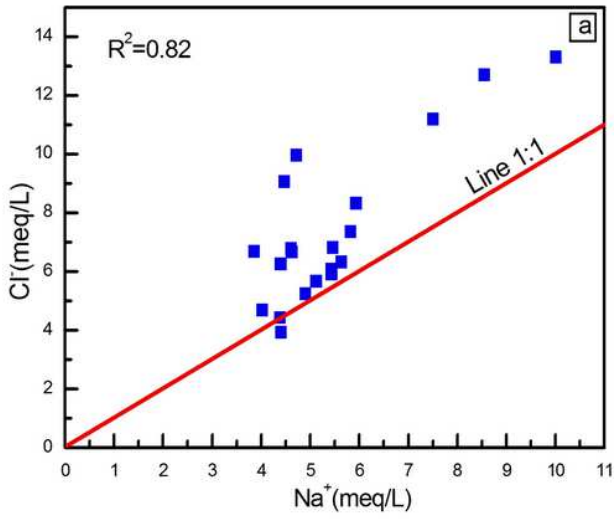


Figure 3

Plots of a Na⁺/Cl⁻, b (Na⁺ + Cl⁻)/ Halite SI

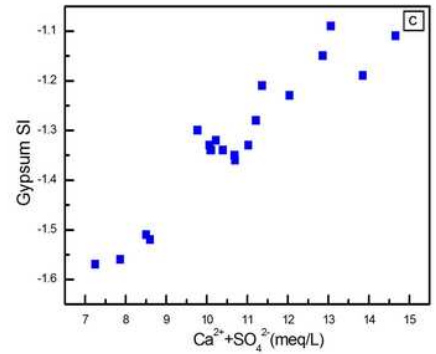
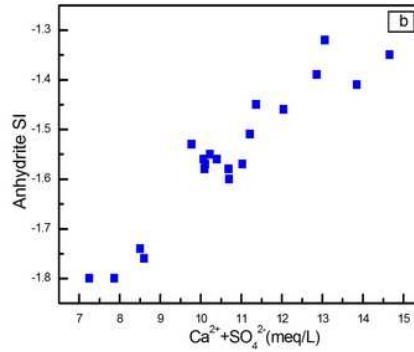
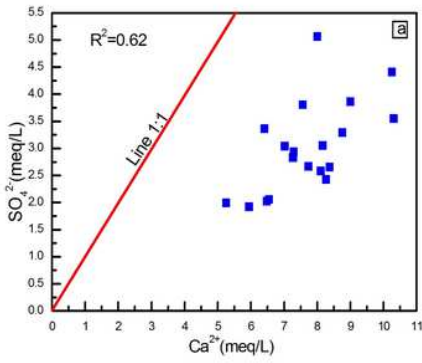


Figure 4

Plots of a Ca²⁺/SO₄²⁻, b (Ca²⁺+SO₄²⁻)/ Anhydrite SI, c (Ca²⁺+SO₄²⁻)/ Gypsum SI

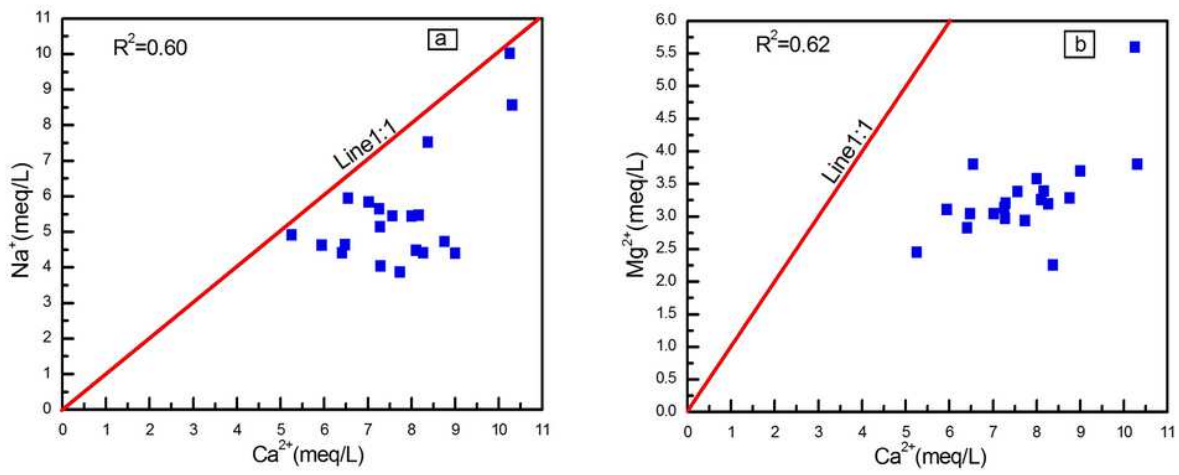


Figure 5

Plots of a $\text{Ca}^{2+}/\text{Na}^+$, b $\text{Ca}^{2+}/\text{Mg}^{2+}$

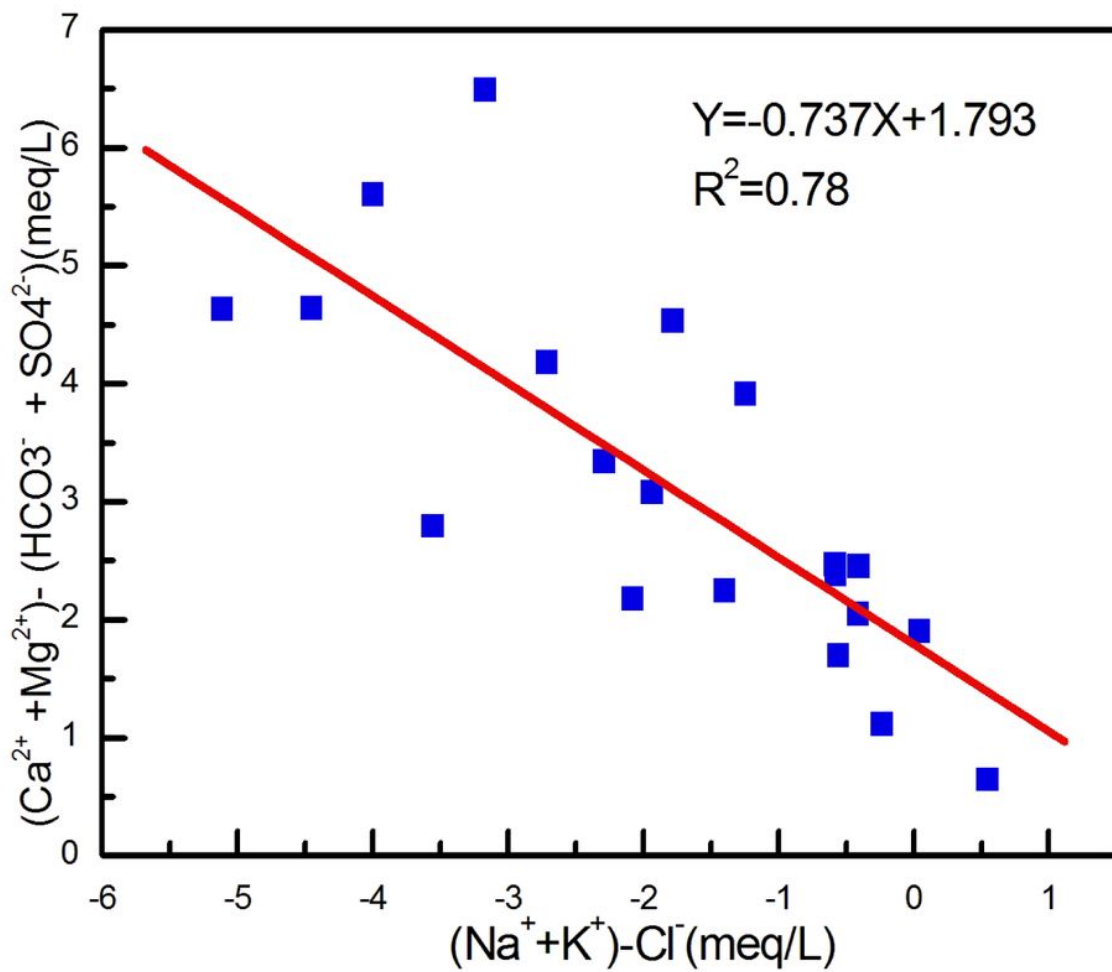


Figure 6

Plot of $(Na^{++}K^{+})-Cl^{-}$ -vs $(Ca^{2++}Mg^{2+}) - (HCO_3^{-} + SO_4^{2-})$

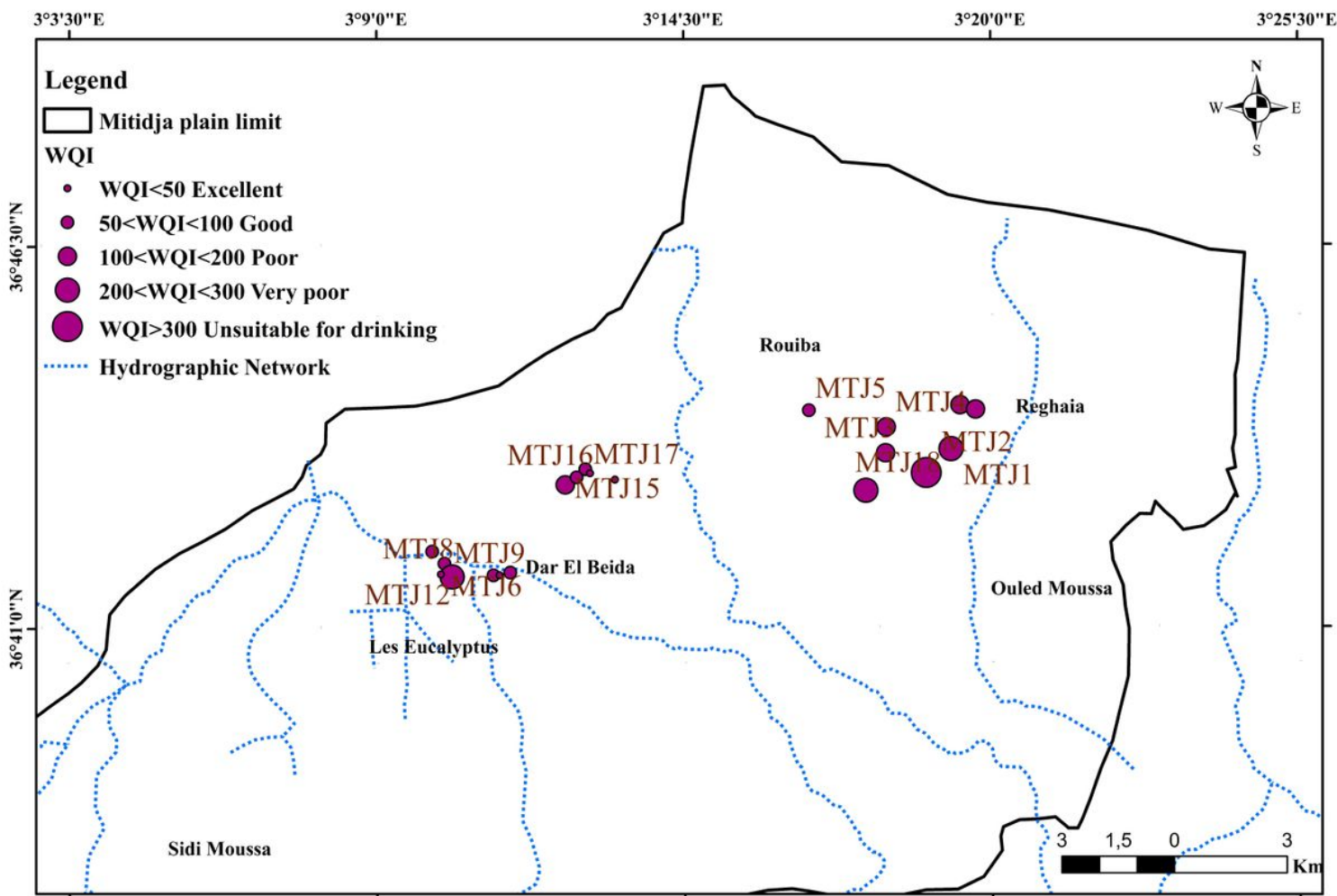


Figure 7

Water Quality Index map of the alluvial aquifer of the Mitidja plain

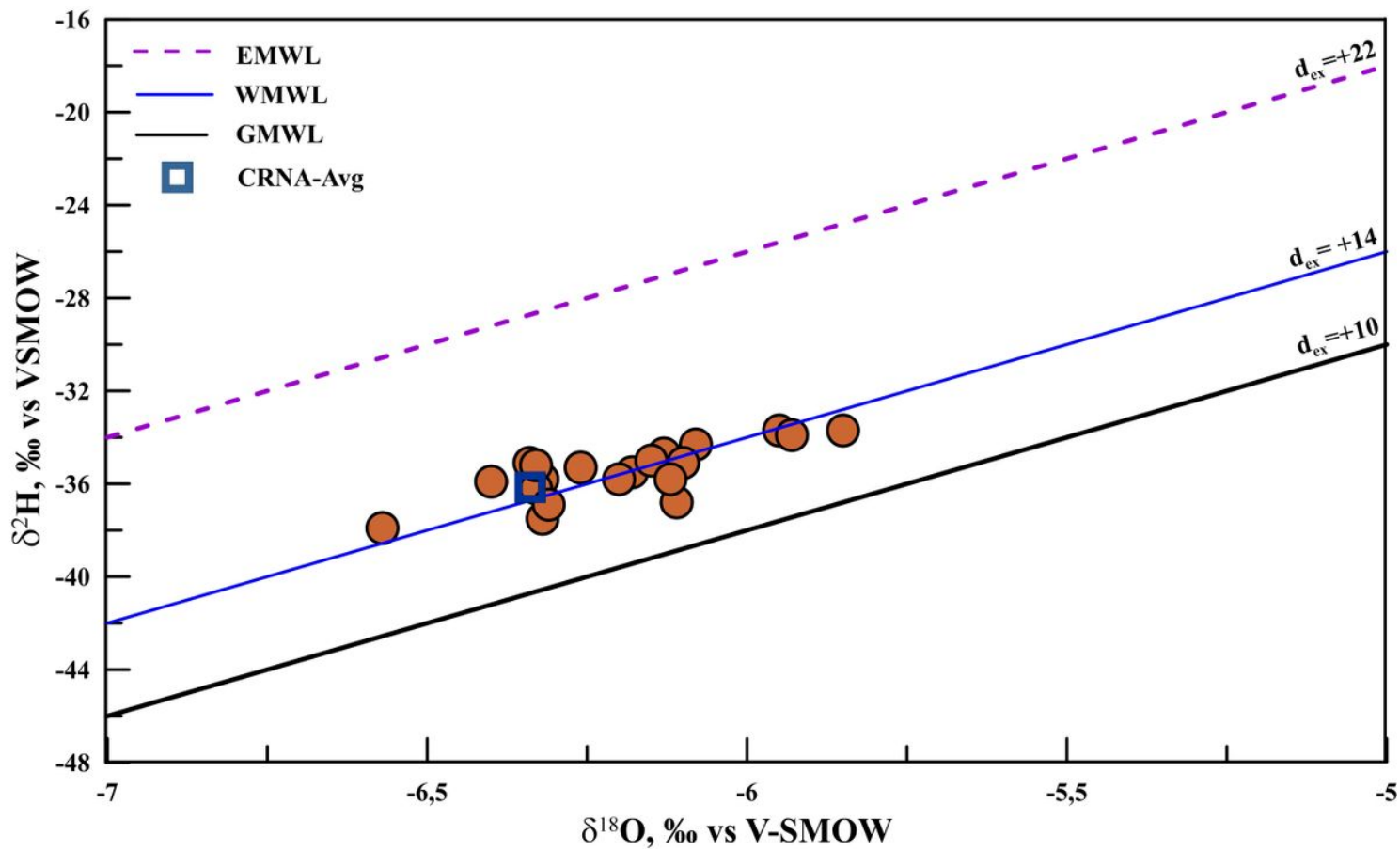


Figure 8

$\delta^{18}\text{O}$ - $\delta^2\text{H}$ plot for groundwater samples from the studied area